

See discussions, stats, and author profiles for this publication at: <https://www.researchgate.net/publication/260137651>

# Crucial Role of H322 in the Folding of Diphtheria Toxin T-Domain into the Open-Channel State

ARTICLE in BIOPHYSICAL JOURNAL · JANUARY 2014

Impact Factor: 3.97 · DOI: 10.1021/bi400249f

CITATIONS

9

READS

26

5 AUTHORS, INCLUDING:



**Mauricio Vargas Uribe**

Universidad Austral de Chile

17 PUBLICATIONS 85 CITATIONS

SEE PROFILE



**Alexey S Ladokhin**

University of Kansas

111 PUBLICATIONS 3,342 CITATIONS

SEE PROFILE

# Crucial Role of H322 in Folding of the Diphtheria Toxin T-Domain into the Open-Channel State

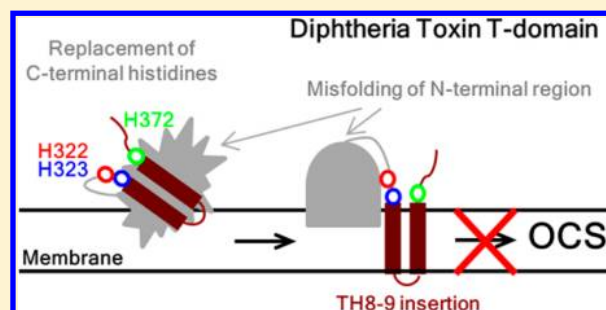
Mauricio Vargas-Urbe,<sup>†</sup> Mykola V. Rodnin,<sup>†</sup> Paul Kienker,<sup>‡</sup> Alan Finkelstein,<sup>‡</sup> and Alexey S. Ladokhin<sup>\*,†</sup>

<sup>†</sup>Department of Biochemistry and Molecular Biology, University of Kansas Medical Center, Kansas City, Kansas 66160, United States

<sup>‡</sup>Department of Physiology and Biophysics, Albert Einstein College of Medicine, Bronx, New York 10461, United States

## Supporting Information

**ABSTRACT:** The translocation (T) domain plays a key role in the entry of diphtheria toxin into the cell. Upon endosomal acidification, the T-domain undergoes a series of conformational changes that lead to its membrane insertion and formation of a channel. Recently, we have reported that the triple replacement of C-terminal histidines H322, H323, and H372 with glutamines prevents the formation of open channels in planar lipid bilayers. Here, we report that this effect is primarily due to the mutation of H322. We further examine the relationship between the loss of functionality and membrane folding in a series of mutants with C-terminal histidine substitutions using spectroscopic assays. The membrane insertion pathway for the mutants differs from that of the wild type as revealed by the membrane-induced red shift of tryptophan fluorescence at pH 6.0–6.5. T-Domain mutants with replacements at H323 and H372, but not at H322, regain a wild-type-like spectroscopic signature upon further acidification. Circular dichroism measurements confirm that affected mutants misfold during insertion into vesicles. Conductance measurements reveal that substituting H322 dramatically reduces the numbers of properly folded channels in a planar bilayer, but the properties of the active channels appear to be unaltered. We propose that H322 plays an important role in the formation of open channels and is involved in guiding the proper insertion of the N-terminal region of the T-domain.



Diphtheria toxin enters the cell via an endosomal pathway, where the translocation domain (T-domain) plays a critical role in cell infection. Upon endosomal internalization, the T-domain undergoes a series of conformational changes in response to the acidification of the endosome, which lead to the insertion of the T-domain into the membrane and the translocation of the catalytic domain into the cytosol.<sup>1</sup> The molecular mechanism of this insertion–translocation pathway, however, is not well understood.

The crystallographic structure of the soluble form of the T-domain at neutral pH<sup>2</sup> reveals the presence of two central hydrophobic helices, TH8 and TH9 (Figure 1A, brown helices), surrounded by seven amphipathic helices (Figure 1A, gray helices). Although no high-resolution structure of the T-domain in its membrane-inserted state is available, multiple studies suggest that helices TH8 and TH9 adopt a trans-membrane topology,<sup>3–7</sup> with a possibility of other regions of the sequence being deeply embedded in the lipid bilayer to form various intermediates,<sup>6–9</sup> as well as the functionally relevant open-channel state (OCS).<sup>5</sup>

The insertion–translocation pathway is modulated by staggered pH-dependent transitions,<sup>10</sup> with several studies implicating the protonation of the six histidines of the T-domain in various stages of the process.<sup>11,12</sup> For example, protonation of H257 has been linked to the early stages of conformational switching, involving the destabilization of the

folded structure of the T-domain in solution and the formation of the membrane-competent state.<sup>13</sup> In contrast, C-terminal histidines H322, H323, and H372, located at the top of the insertion unit of TH8 and TH9 (color-coded in Figure 1A), affect the later stages of the folding in the membrane.<sup>14</sup> Recently, we have reported that a triple substitution of these residues does not affect the insertion of the TH8–TH9 domain but does affect the physiological activity of the T-domain.<sup>14</sup> That study raised two important questions. (1) Why does the replacement of C-terminal histidines result in a loss of activity despite the apparently normal interactions with the lipid bilayer? (2) Are any of the three histidines more important than the others, or will single and double replacements show a cumulative effect? In this study, we addressed these questions by generating a series of mutants of the C-terminal histidines and testing their ability to effectively fold into an OCS. Spectroscopic and conductivity measurements indicate a strong correlation between the inability to form the OCS and the misfolding of the T-domain in the membrane and reveal a critical role of H322 in the folding process.

**Received:** February 27, 2013

**Revised:** April 24, 2013



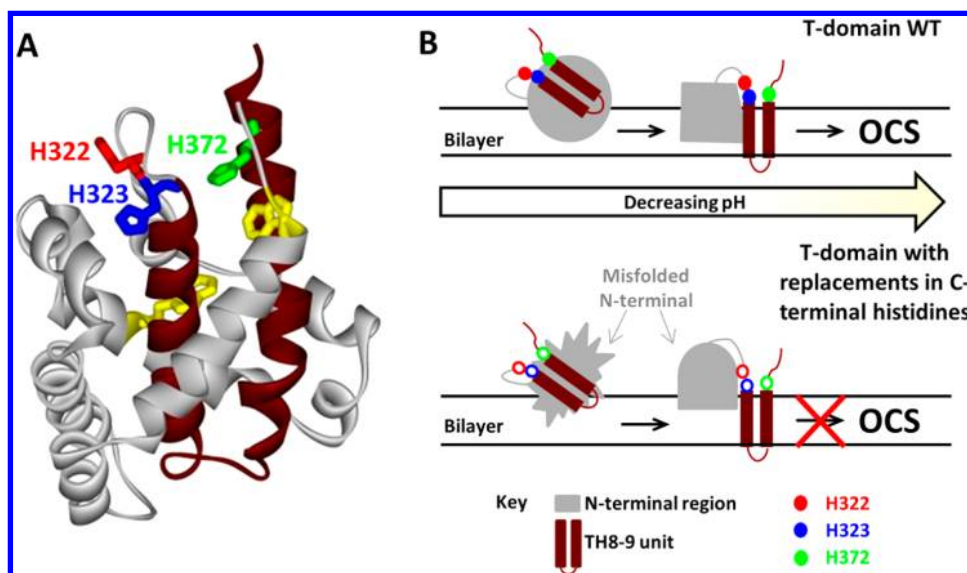


**Figure 1.** (A) Crystal structure of the soluble form of the diphtheria toxin T-domain at neutral pH.<sup>2</sup> C-Terminal histidines H322, H323, and H372 are color-coded. The insertion unit comprised of a helical hairpin (TH8 and TH9) is colored brown. Tryptophan residues W206 and W281 are colored yellow, and the rest of the protein is colored gray. (B) Model of the role of the C-terminal histidines in the refolding process of the T-domain within the bilayer. In the top panel (WT T-domain), upon initial destabilization of the WT T-domain and its association with the lipid bilayer, the N-terminal region of the protein adopts a conformation that leads to the insertion of TH8 and TH9 into the bilayer. The N-terminal region refolds to form the OCS. In the bottom panel (mutants with C-terminal histidine replacements), membrane interaction of these mutants results in a conformation different from that of the WT, specifically in the more exposed N-terminal part as revealed by a red-shifted fluorescence. While the insertion of TH8 and TH9 is not compromised,<sup>14</sup> replacement of C-terminal histidines, especially H322, affects efficient folding of the T-domain into the OCS (see the text for details).

## MATERIALS AND METHODS

**Materials.** POPC, POPG, POPS, and POPE were purchased from Avanti Polar Lipids (Alabaster, AL). The diphtheria toxin T-domain (amino acids 202–378) was cloned into the NdeI- and EcoRI-treated pET15b vector containing an N-terminal six-His tag and a thrombin cleavage site. Both the mutants and the WT protein were expressed and purified as described in ref 15.

**Conductance Assays in Planar Bilayers.** The current response was measured under voltage-clamp conditions in planar phospholipid bilayers separating two compartments: the cis compartment with acidic buffer into which the proteins were injected from a stock solution and the trans compartment with neutral buffer, as previously described.<sup>16</sup> Asolectin planar bilayers were formed, and voltage-clamp recordings were performed as previously described.<sup>17</sup> The voltage is defined as the potential of the cis compartment, relative to that of the opposite trans compartment. Both aqueous solutions contained 1 M KCl, 2 mM CaCl<sub>2</sub>, and 1 mM EDTA; in addition, the cis compartment contained 20 mM malic acid (pH 5.3), and the trans compartment contained 20 mM HEPES (pH 7.2).

**LUV Preparation.** Large unilamellar vesicles (LUV) 0.1  $\mu$ m in diameter were prepared by extrusion as previously described.<sup>18,19</sup> The vesicles were composed of molar mixtures of POPG and POPC (3:1), POPG and POPC (1:3), POPG and POPE (3:1), and POPS and POPC (3:1).

**Tryptophan Fluorescence Measurements.** Fluorescence was measured using a SPEX Fluorolog FL3-22 steady-state fluorescence spectrometer (Jobin Yvon, Edison, NJ) equipped with double grating. The measurements were taken at 25 °C in 2 mm  $\times$  10 mm cuvettes oriented perpendicular to the excitation beam. Tryptophan residues were excited at 280 nm, and the emission spectra were recorded between 290 and 500

nm using excitation and emission spectral slits of 2 and 4 nm, respectively. Normally, we added purified WT or mutant T-domain from a concentrated stock to 50 mM sodium phosphate buffer (pH 8.0). We then mixed the sample with LUV to reach final T-domain and lipid concentrations of 1  $\mu$ M and 1 mM, respectively, and the rapid acidification was achieved by addition of small amounts of concentrated acetic buffer. We recorded at least five scans after an incubation time of 30 min to ensure the equilibration of the sample. All spectra were corrected for background and fit to a log-normal distribution as described in ref 20 to determine the position of maximal emission. Normally, positions of maxima for three to six samples were averaged.

**CD Measurements and Analysis of Thermal Unfolding.** CD measurements were performed using an upgraded Jasco-720 spectropolarimeter (Japan Spectroscopic Co., Tokyo, Japan). Normally, 100 scans were recorded between 190 and 260 nm with a 1 nm step at 25 °C, using a 1 mm optical path cuvette. The sample contained 4  $\mu$ M T-domain, either WT or mutant, and 1 mM lipid in 50 mM phosphate buffer (pH 8.0). The rapid acidification was achieved as described for the fluorescence experiments. All spectra were corrected for background; however, only the data collected at wavelengths longer than 200 nm, where effects of scattering are negligible,<sup>21</sup> are presented. The thermal unfolding of the WT and mutant T-domain in solution at pH 8.0 and 6.0 was measured at 222 nm with a scan rate of 1 °C/min. The analysis of thermal stability, yielding transition temperature  $T_m$  and transition enthalpy  $\Delta H^\circ$ , was performed as described previously.<sup>14</sup>

## RESULTS AND DISCUSSION

In our previous study, we demonstrated that a triple replacement of all C-terminal histidines in the T-domain affects the formation of the OCS by uncoupling the insertion of

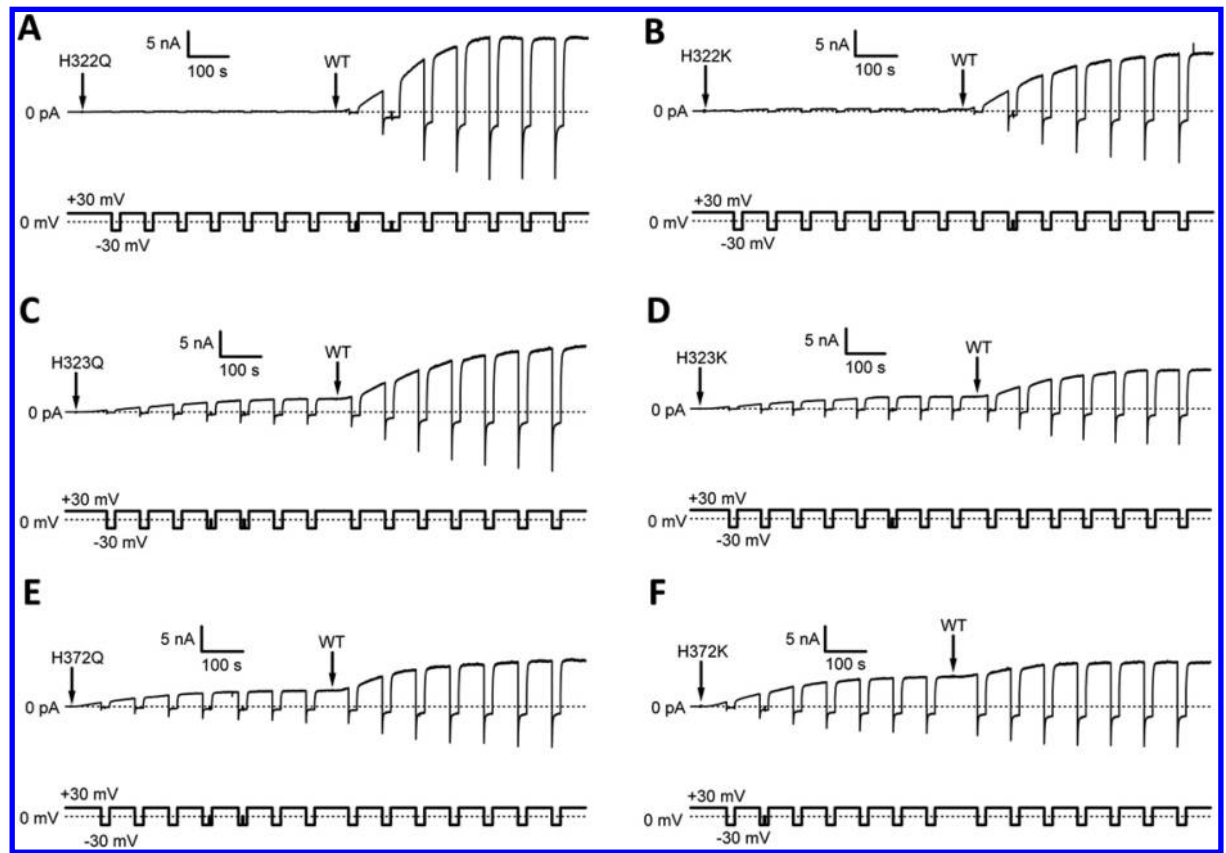


**Figure 2.** Functional assay of H322, H323, and H372 mutants measured in planar bilayers via electrophysiology as previously described.<sup>16</sup> Briefly, the transmembrane current (top traces) was measured at  $\pm 30$  mV (bottom traces) in the presence of 150 pM mutant T-domain in the cis compartment at pH 5.3 (first arrow) and followed by the addition of 150 pM WT T-domain (second arrow). The replacement of H322 with either glutamine or lysine (panels A and B) resulted in a dramatic loss of the ability to permeabilize the planar bilayer, whereas the substitution of H323 (C and D) and H372 (E and F) did not greatly affect the activity of the T-domain.

the TH8–TH9 helical hairpin (colored brown in Figure 1A) from the translocation of the N-terminus across the lipid bilayer.<sup>14</sup> Here we examine the role of individual histidines in the formation of the OCS by replacing them one at a time with either lysine or glutamine. First, we tested their activity by measuring the conductance in a planar lipid bilayer as described previously.<sup>14,16,17</sup> As shown in Figure 2, the addition of any of the single-histidine mutants to the low-pH cis compartment (first arrow) generally caused a smaller increase in the conductance than that of the WT T-domain (second arrow). The mutation of H322 resulted in the most dramatic effect, as the activities of both H322Q and H322K were almost undetectable (Figure 2A,B). Indeed, the relative activities of these mutants were 2 orders of magnitude lower than that of the WT T-domain (Table 1). The effect of substituting H323 and H372 (Figure 2C–F) was less pronounced, resulting in relative activities within a factor of 4 of that of the WT T-domain (Table 1). A closer look at the current–voltage dependence, even of the least active mutant H322Q (see Figure S1 of the Supporting Information), reveals the characteristic blocking of the channels by the His tag when a negative potential was applied.<sup>5</sup> Thus, the loss of activity is likely to be associated with a reduction in the number of channels rather than with changes in the properties of the individual channel. These results suggest that each of the three C-terminal histidines affects the formation of the OCS, but the role of H322 appears to be critical.

**Table 1. Relative Activities of the C-Terminal Histidine Mutants of the Diphtheria Toxin T-Domain<sup>a</sup>**

T-domain	relative activity
WT	1
H322K	0.028 $\pm$ 0.004
H322Q	0.011 $\pm$ 0.005
H323K	0.38 $\pm$ 0.06
H323Q	0.26 $\pm$ 0.04
H372K	0.83 $\pm$ 0.09
H372Q	0.41 $\pm$ 0.04
H322,323Q	0.007
H322,323,372Q	0.002

<sup>a</sup>The values are calculated relative to the total increase in the conductance of the WT. For the single replacements, the values correspond to the average and standard deviation of three independent assays.

The refolding–insertion pathway of the T-domain is initiated by the acid-induced destabilization of the folded membrane-incompetent state and the formation of the membrane-competent state, a partially refolded intermediate capable of interaction with membranes.<sup>10</sup> While the triple replacement of C-terminal histidines does not appear to affect the thermodynamic stability of the membrane-incompetent state,<sup>14</sup> the effect on the stability of the membrane-competent state has not been explored. Here, we examine the stability of the WT and mutant proteins by measuring temperature-dependent changes in



ellipticity associated with the helical structure using CD spectroscopy. The data collected at pH 8 and 6 (Figure 3),

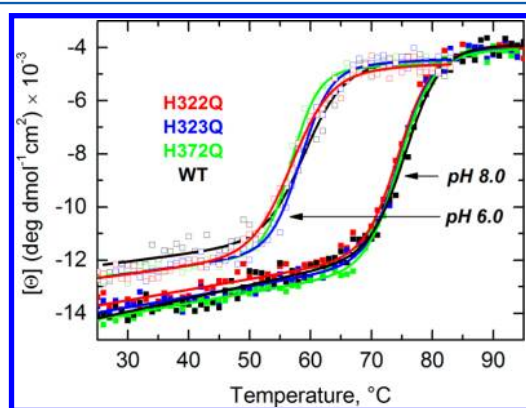


**Figure 3.** Thermal stability of H322Q, H323Q, and H372Q mutants at pH 8 and 6 measured by CD spectroscopy. The loss of secondary structure induced by an increase in temperature at pH 8 (filled symbols) or pH 6 (empty symbols) was followed at 222 nm. Lines represent the fitting curves obtained as described in ref 14, and the values for enthalpies and transition temperatures are summarized in Table S1 of the Supporting Information. None of the replacements (color-coded as in Figure 1) caused a noticeable change in stability compared to that of the WT protein (black) at either pH, confirming that the replacement of C-terminal histidines does not alter the acid destabilization process in solution.

corresponding to membrane-incompetent and membrane-competent states, respectively, indicate a very similar behavior for all proteins. Mild acidification results in a similar reduction in the transition temperature and enthalpy (Table S1 of the Supporting Information). No reproducible data, however, could be collected at lower pH values, as the protein aggregation in the denatured state renders thermodynamic analysis impossible. Nevertheless, it is clear that the reason for the loss of functional activity due to histidine replacements is not associated with changes in stability in solution but is rather related to altered interactions with the membranes at some point along the insertion pathway.

Previously, we demonstrated that triple substitutions of C-terminal histidines do not prevent efficient insertion of the TH8–TH9 helical hairpin<sup>14</sup> (brown helices in Figure 1A), suggesting that they affect the proper insertion of the rest of the structure (gray helices in Figure 1A). Here we follow up on this result using the intrinsic fluorescence from W206 and W281, located in N-terminal helices TH1 and TH5, respectively (yellow in Figure 1A). Representative examples of fluorescence spectra of the WT and H322Q mutant of the T-domain are shown as empty symbols in Figure 4. Although the spectra in the membrane-incompetent state are superimposable (panel A), there is a pronounced difference when WT and the mutant interact with the membrane (panel B). To accurately measure spectral shifts, fluorescence spectra are fit to a log-normal distribution (fits are shown as solid lines), as described in Materials and Methods. This procedure allows for accurate and reliable measurements of subtle changes in the tryptophan spectral position.<sup>20</sup>

Complementing our thermal stability CD results, the spectral position of the Trp fluorescence maximum in solution is not affected by the mutations at any pH value tested (e.g., compare H322Q and H322K with WT in Figure 5A). On the other hand, the mutants show a distinct red shift of emission in the

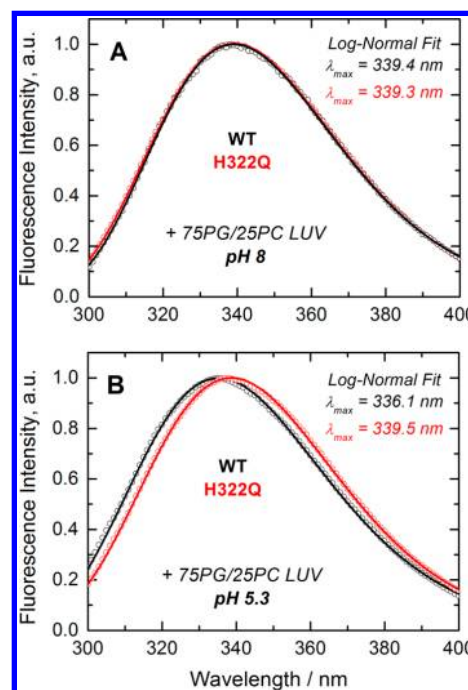


**Figure 4.** Tryptophan spectra of WT and H322Q mutants in the presence of LUV at pH 8 (A) and 5.3 (B). All spectra (empty symbols) were corrected for background, normalized to the maximal intensity for visual comparison of spectral changes, and fit to a log-normal function (lines) according to Ladokhin et al.<sup>20</sup> to estimate the position of the maximum.

presence of membranes, normally associated with an increased level of exposure of fluorophores to the aqueous phase (Figure 5B–D). These changes are detected at all lipid compositions that we tested and appear to be exactly the same for 3:1 anionic lipid/neutral lipid mixtures, regardless of the substitution of PC with PE, or PG with PS (Figure 5C). At lower anionic contents, the same effect is observed, but the curves are shifted to more acidic pH values (Figure 5D). These changes are indicative of a membrane-induced misfolding of intermediate states on the path toward the OCS.

As illustrated in Figure 6A, this misfolding-associated red shift in Trp fluorescence occurs at pH 6.0–6.5 in all mutants, including those with substitutions of H323 and H372. The latter mutants regain the WT-like spectroscopic signature at pH 5.3 (blue and green symbols) and are relatively active in the electrophysiological assay (Table 1). Mutants with replacements of H322 (red, orange, and magenta symbols), however, do not show a WT-like spectral shift at lower pH values and are inactive. It is possible that fluorescence spectra for these mutants will be blue-shifted under more acidic conditions; however, this will not be physiologically relevant.

To corroborate the fact that the inactive mutants adopted a misfolded conformation within the bilayer, we recorded the CD spectra of the WT T-domain and the active and inactive mutants in the presence of LUV (3:1 POPG/POPC LUV) at pH 5.3 (Figure 6B). The CD spectra of the membrane-inserted state of the WT T-domain (black spectrum) and the active mutant H372Q (green spectrum) are identical and exhibit the characteristics of an  $\alpha$ -helical structure, with two minima at 222 and 208 nm. In contrast, inactive mutants H322Q (red spectrum), H322,323Q (orange spectrum), and H322,323,372Q (magenta spectrum) showed CD spectra

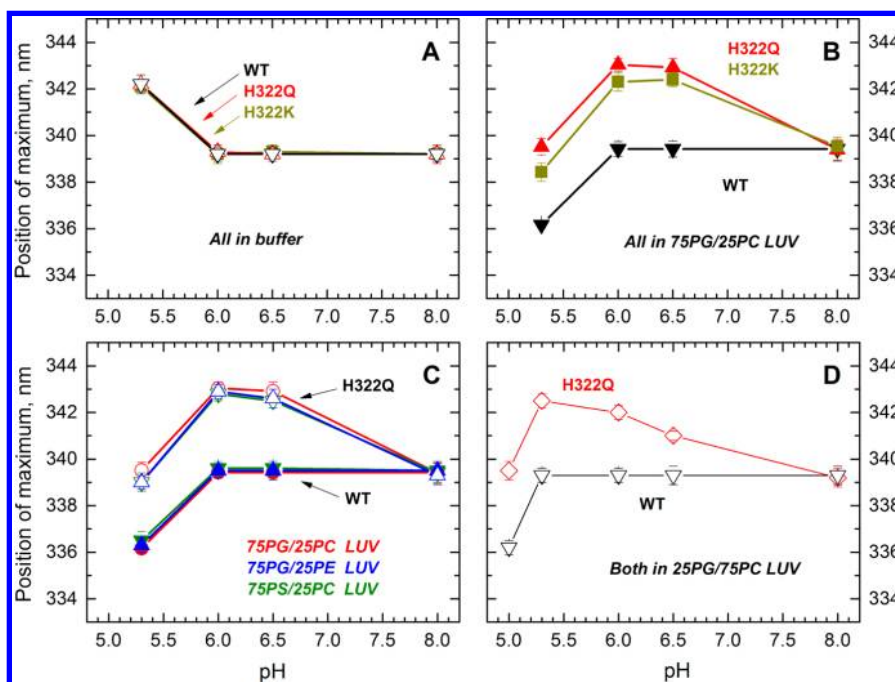


**Figure 5.** Membrane-induced misfolding of the T-domain mutants with replaced H322 detected by Trp fluorescence. (A and B) Positions of maxima of intrinsic fluorescence emission as a function of pH for the WT T-domain and H322Q and H322K mutants in the absence of LUV (A) or in the presence of 75:25 POPG/POPC LUV (B). The presence of membranes induces the red shift of the tryptophan emission spectrum at pH 6–6.5 for the mutants, whereas further acidification induces the blue shift of the spectra for the WT and mutant T-domain. The final state adopted by the mutants is different from that adopted by the WT T-domain. (C and D) Positions of maxima of intrinsic fluorescence emission as a function of pH for the WT T-domain and mutant H322Q in LUV composed of POPG and POPC (75:25), POPG and POPE (75:25), POPS and POPC (75:25) (C), and POPG and POPC (25:75) (D). The effect of replacing H322 on the emission spectra is maintained regardless of the composition of the LUV. Error bars represent the standard deviation of at least three independent measurements.

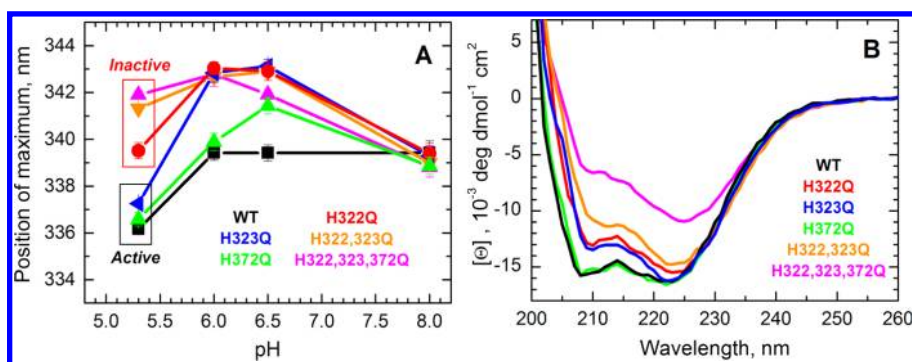


**Figure 6.** Folding of the T-domain C-terminal histidine mutants followed by Trp fluorescence (A) and CD (B). (A) Wavelengths of maximal tryptophan emission represented as a function of pH for active and inactive mutants in the presence of LUV. All of the mutants show red-shifted spectra at pH 6–6.5. At pH 5.3, the spectra are blue-shifted for the active mutants (black box), but not in the case of the inactive mutants (red box). (The spectra of the double and triple mutants are even red-shifted relative to the pH 8 spectra.) The error bars represent the standard deviation of three independent measurements. (B) CD spectra of the WT T-domain and representative active and inactive mutants at pH 5.3 in the presence of LUV. The inactive mutants show an atypical CD spectral shape and a decrease in ellipticity.

with loss of ellipticity and characteristic changes in shape, associated with the misfolding and aggregation of membrane proteins,<sup>22,23</sup> indicating that they do not fold into a WT-like structure. Previously, we demonstrated that noninserted intermediates of another protein that undergoes pH-dependent membrane insertion, annexin B12, are prone to aggregation on the interfaces.<sup>24,25</sup> The relatively active mutant, H323Q (blue spectrum), does not quite follow this pattern; it has a CD spectrum similar to that of the inactive mutant H322Q. Fluorescence data indicate that H323Q is strongly misfolded at the intermediate pH of 6.0 yet inserts like the WT at pH 5.3 (Figure 6A). The likely reason why it cannot regain a proper

fold under the conditions of the CD experiment is that the latter requires concentrations much higher than those used in fluorescence or conductance measurements. Indeed, when the concentration of this mutant in the tryptophan fluorescence assay was increased, the spectrum no longer returned to the WT position (data not shown).

## SUMMARY

We illustrate our findings in the scheme (Figure 1B) summarizing membrane insertion of the WT T-domain (top panel) and the mutants carrying substitutions of the C-terminal histidines (bottom panel). Upon the initial formation of the

membrane-competent state and binding to the membrane, the process continues through the insertion of TH8 and TH9 into the bilayer and the subsequent refolding of the rest of the protein until it reaches the open-channel state.<sup>10</sup> In the case of the WT protein, we propose that the C-terminal histidines are involved in guiding the conformation of the N-terminal region through productive folding intermediate states toward the OCS. There is no high-resolution structure of the OCS available (or that of any membrane-associated intermediate); however, the electrophysiological data are consistent with helices TH8, TH9, and TH5 adopting a transmembrane conformation.<sup>5</sup> When C-terminal histidines are replaced, the protein still undergoes a proper pH-dependent destabilization in solution (Figure 3), binds to membranes (Figure S2 of the Supporting Information), and inserts a TH8–TH9 helical hairpin<sup>14</sup> similar to that of the WT (Figure 1B, bottom panel). Histidine replacement, however, leads to the formation of a nonproductive intermediate that is characterized by greater exposure of W206 and W281 to the aqueous phase at pH ~6–6.5, manifesting itself in red-shifted fluorescence spectra (Figures 5 and 6). The replacement of H322 appears to be particularly damaging, as the corresponding mutants tend to misfold on the membrane, dramatically reducing the number of properly folded and functional channels (Figure 2 and Figure S1 of the Supporting Information). Interestingly, the replacement of H322 with the charged lysine or neutral glutamine has a similar effect on the folding pathway (Figure 5B). (This is different from replacements of another critical residue, H257, involved in destabilization of the folded structure in solution.<sup>13</sup> While replacement of H257 with a charged residue promoted unfolding, replacement with a neutral residue slowed it.) Thus, we propose that the C-terminal histidines play a crucial role in guiding the folding of the N-terminal region into the OCS, where residue H322 would have particular importance that likely goes beyond its mere protonation.

## ■ ASSOCIATED CONTENT

### ● Supporting Information

Two figures and a table. This material is available free of charge via the Internet at <http://pubs.acs.org>.

## ■ AUTHOR INFORMATION

### Corresponding Author

\*E-mail: [aladokhin@kumc.edu](mailto:aladokhin@kumc.edu). Phone: (913) 588-0489. Fax: (913) 588-7440.

### Funding

This research was supported by National Institutes of Health Grants GM-069783 (A.S.L.) and GM-29210 (A.F.). M.V.-U. was supported in part by Fulbright-CONICYT.

### Notes

The authors declare no competing financial interest.

## ■ ABBREVIATIONS

T-domain, diphtheria toxin T-domain; WT, wild type (T-domain); CD, circular dichroism; LUV, large unilamellar vesicles; POPC, palmitoylcholinephosphatidylcholine; POPG, palmitoylcholinephosphatidylglycerol; POPE, palmitoylcholinephosphatidylethanolamine; POPS, palmitoylcholinephosphatidylserine; OCS, open-channel state.

## ■ REFERENCES

- (1) Murphy, J. R. (2011) Mechanism of diphtheria toxin catalytic domain delivery to the eukaryotic cell cytosol and the cellular factors that directly participate in the process. *Toxins (Basel)* 3, 294–308.
- (2) Bennett, M. J., and Eisenberg, D. (1994) Refined structure of monomeric diphtheria toxin at 2.3 Å resolution. *Protein Sci.* 3, 1464–1475.
- (3) Oh, K. J., Zhan, H., Cui, C., Altenbach, C., Hubbell, W. L., and Collier, R. J. (1999) Conformation of the diphtheria toxin T domain in membranes: A site-directed spin-labeling study of the TH8 helix and TL5 loop. *Biochemistry* 38, 10336–10343.
- (4) Oh, K. J., Zhan, H., Cui, C., Hideg, K., Collier, R. J., and Hubbell, W. L. (1996) Organization of diphtheria toxin T domain in bilayers: A site-directed spin labeling study. *Science* 273, 810–812.
- (5) Senzel, L., Gordon, M., Blaustein, R. O., Oh, K. J., Collier, R. J., and Finkelstein, A. (2000) Topography of diphtheria toxin's T domain in the open channel state. *J. Gen. Physiol.* 115, 421–434.
- (6) Rosconi, M. P., Zhao, G., and London, E. (2004) Analyzing topography of membrane-inserted diphtheria toxin T domain using BODIPY-streptavidin: At low pH, helices 8 and 9 form a transmembrane hairpin but helices 5–7 form stable nonclassical inserted segments on the cis side of the bilayer. *Biochemistry* 43, 9127–9139.
- (7) Kachel, K., Ren, J., Collier, R. J., and London, E. (1998) Identifying transmembrane states and defining the membrane insertion boundaries of hydrophobic helices in membrane-inserted diphtheria toxin T domain. *J. Biol. Chem.* 273, 22950–22956.
- (8) Wang, Y., Kachel, K., Pablo, L., and London, E. (1997) Use of Trp mutations to evaluate the conformational behavior and membrane insertion of A and B chains in whole diphtheria toxin. *Biochemistry* 36, 16300–16308.
- (9) Wang, Y., Malenbaum, S. E., Kachel, K., Zhan, H., Collier, R. J., and London, E. (1997) Identification of shallow and deep membrane-penetrating forms of diphtheria toxin T domain that are regulated by protein concentration and bilayer width. *J. Biol. Chem.* 272, 25091–25098.
- (10) Kyrychenko, A., Posokhov, Y. O., Rodnin, M. V., and Ladokhin, A. S. (2009) Kinetic intermediate reveals staggered pH-dependent transitions along the membrane insertion pathway of the diphtheria toxin T-domain. *Biochemistry* 48, 7584–7594.
- (11) Ladokhin, A. S., Legmann, R., Collier, R. J., and White, S. H. (2004) Reversible refolding of the diphtheria toxin T-domain on lipid membranes. *Biochemistry* 43, 7451–7458.
- (12) Perier, A., Chassaing, A., Raffestin, S., Pichard, S., Masella, M., Menez, A., Forge, V., Chenal, A., and Gillet, D. (2007) Concerted protonation of key histidines triggers membrane interaction of the diphtheria toxin T domain. *J. Biol. Chem.* 282, 24239–24245.
- (13) Rodnin, M. V., Kyrychenko, A., Kienker, P., Sharma, O., Posokhov, Y. O., Collier, R. J., Finkelstein, A., and Ladokhin, A. S. (2010) Conformational switching of the diphtheria toxin T domain. *J. Mol. Biol.* 402, 1–7.
- (14) Rodnin, M. V., Kyrychenko, A., Kienker, P., Sharma, O., Vargas-Urbe, M., Collier, R. J., Finkelstein, A., and Ladokhin, A. S. (2011) Replacement of C-terminal histidines uncouples membrane insertion and translocation in diphtheria toxin T-domain. *Biophys. J.* 101, L41–L43.
- (15) Rodnin, M. V., Posokhov, Y. O., Contino-Pepin, C., Brettmann, J., Kyrychenko, A., Palchevskyy, S. S., Pucci, B., and Ladokhin, A. S. (2008) Interactions of fluorinated surfactants with diphtheria toxin T-domain: Testing new media for studies of membrane proteins. *Biophys. J.* 94, 4348–4357.
- (16) Senzel, L., Huynh, P. D., Jakes, K. S., Collier, R. J., and Finkelstein, A. (1998) The diphtheria toxin channel-forming T domain translocates its own NH<sub>2</sub>-terminal region across planar bilayers. *J. Gen. Physiol.* 112, 317–324.
- (17) Kienker, P. K., Jakes, K. S., and Finkelstein, A. (2000) Protein translocation across planar bilayers by the colicin Ia channel-forming domain: Where will it end? *J. Gen. Physiol.* 116, 587–598.

- (18) Mayer, L. D., Hope, M. J., and Cullis, P. R. (1986) Vesicles of variable sizes produced by a rapid extrusion procedure. *Biochim. Biophys. Acta* 858, 161–168.
- (19) Hope, M., Bally, M., Mayer, L., Janoff, A., and Cullis, P. (1986) Generation of multilamellar and unilamellar phospholipid vesicles. *Chem. Phys. Lipids* 40, 89–107.
- (20) Ladokhin, A. S., Jayasinghe, S., and White, S. H. (2000) How to measure and analyze tryptophan fluorescence in membranes properly, and why bother? *Anal. Biochem.* 285, 235–245.
- (21) Ladokhin, A. S., Fernandez-Vidal, M., and White, S. H. (2010) CD spectroscopy of peptides and proteins bound to large unilamellar vesicles. *J. Membr. Biol.* 236, 247–253.
- (22) Wallace, B. A., and Teeters, C. L. (1987) Differential absorption flattening optical effects are significant in the circular dichroism spectra of large membrane fragments. *Biochemistry* 26, 65–70.
- (23) Glaeser, R. M., and Jap, B. K. (1985) Absorption flattening in the circular dichroism spectra of small membrane fragments. *Biochemistry* 24, 6398–6401.
- (24) Ladokhin, A. S. (2008) Insertion intermediate of annexin B12 is prone to aggregation on membrane interfaces. *Biopolym. Cell* 24, 101–104.
- (25) Posokhov, Y. O., Rodnin, M. V., Lu, L., and Ladokhin, A. S. (2008) Membrane insertion pathway of annexin B12: Thermodynamic and kinetic characterization by fluorescence correlation spectroscopy and fluorescence quenching. *Biochemistry* 47, 5078–5087.